

## Electronic Structures of Scandium Oxide Endohedral Metallofullerenes, $\text{Sc}_4(\mu_3\text{-O})_n@I_h\text{-C}_{80}$ ( $n = 2, 3$ )

Ramón Valencia,<sup>†</sup> Antonio Rodríguez-Fortea,<sup>†</sup> Steven Stevenson,<sup>‡</sup> Alan L. Balch,<sup>\*§</sup> and Josep M. Poble<sup>t\*</sup>

<sup>†</sup>Departament de Química Física i Inorgànica, Universitat Rovira i Virgili, c/ Marcel·lí Domingo s/n, 43007 Tarragona, Spain, <sup>‡</sup>Department of Chemistry, University of Southern Mississippi, Hattiesburg, Mississippi 39406, and <sup>§</sup>Department of Chemistry, University of California, One Shields Avenue, Davis, California 95616

Received February 20, 2009

Density functional theory computations for  $\text{Sc}_4(\mu_3\text{-O})_2@I_h\text{-C}_{80}$  and  $\text{Sc}_4(\mu_3\text{-O})_3@I_h\text{-C}_{80}$  (which is more stable than the alternative  $\text{Sc}_4(\mu_3\text{-O})_2@I_h\text{-C}_{80}\text{O}$ ) reveal that the electronic structures of these two Sc-oxide endohedral metallofullerenes are different.  $\text{Sc}_4(\mu_3\text{-O})_2@I_h\text{-C}_{80}$  involves a mixed valence cluster with the highest occupied molecular orbital (HOMO) localized on the metal cluster while in  $\text{Sc}_4(\mu_3\text{-O})_3@I_h\text{-C}_{80}$  the HOMO is localized on the carbon cage and the electronic structure resembles that of  $\text{Sc}_3\text{N}@I_h\text{-C}_{80}$ .

### Introduction

Endohedral fullerenes are now known that contain metal nitride,<sup>1</sup> metal carbide,<sup>2</sup> and metal oxide<sup>3</sup> clusters trapped within closed cages of carbon atoms. Currently,  $\text{Sc}_4(\mu_3\text{-O})_2@I_h\text{-C}_{80}$ , whose structure is shown in Figure 1, contains the largest known cluster to have been trapped inside a fullerene. Here we report density functional theory (DFT) computations of the electronic structure of  $\text{Sc}_4(\mu_3\text{-O})_2@I_h\text{-C}_{80}$  and  $\text{Sc}_4\text{O}_3\text{C}_{80}$ . For the latter compound, whose structure is not determined yet, two likely structures, as proposed by Stevenson and Balch,<sup>3</sup> have been investigated:  $\text{Sc}_4(\mu_3\text{-O})_3@I_h\text{-C}_{80}$ , with the additional O atom as a part of the internal cluster, and  $\text{Sc}_4(\mu_3\text{-O})_2@I_h\text{-C}_{80}\text{O}$ , with the O atom forming an exohedral epoxide group.

### Computational Details

All the calculations were carried out using the ADF 2007 code.<sup>4</sup> The exchange-correlation functionals of Becke and

Perdew were used.<sup>5</sup> Relativistic corrections were included by means of the ZORA formalism. Triple- $\zeta$  polarization basis sets were employed to describe the valence electrons of the C, O, and Sc atoms. Frozen cores consisting of (i) the 1s shell for C, O; and (ii) the 1s to 2p shells for Sc were described by means of single Slater functions. The calculations for predicting the electrochemical (EC) gap were done in the presence of a continuous model solvent by means of the conductor-like screening model (COSMO)<sup>6</sup> implemented in the ADF code.<sup>7</sup> To define the cavity that surrounds the molecules we use the solvent excluding surface (SES) method and a fine tesserae. The radii of the atoms, which define the dimensions of the cavity surrounding the molecule, are chosen to be 1.00 Å for Sc, 1.55 for O, and 1.70 for C. The dielectric constant is set to 9.8 so as to model *o*-dichlorobenzene (*o*-dcb) as solvent. The EC gaps are computed as the difference between the oxidation energy and the absolute value of the reduction energy in *o*-dcb without taking into account neither thermal nor entropic effects. This approximation has been shown to predict more than acceptably the EC gaps for the family of metal nitride endohedral fullerenes (MNEFs)<sup>8</sup> as well as in more complex systems.<sup>9</sup>

### Results and Discussion

**Electronic Structure of  $\text{Sc}_4(\mu_3\text{-O})_2@I_h\text{-C}_{80}$ .** The structures of nine isomers of  $\text{Sc}_4(\mu_3\text{-O})_2@I_h\text{-C}_{80}$ , in which the

\*To whom correspondence should be addressed. E-mail: josepmaria.poblet@urv.cat (J.M.P.), albalch@ucdavis.edu (A.L.B.).

(1) Stevenson, S.; Rice, G.; Glass, T.; Harich, K.; Cromer, F.; Jordan, M. R.; Craft, J.; Hadju, E.; Bible, R.; Olmstead, M. M.; Maitra, K.; Fisher, A. J.; Balch, A. L.; Dorn, H. C. *Nature* **1999**, *401*, 55.

(2) (a) Iiduka, Y.; Wakahara, T.; Nakahodo, T.; Tsuchiya, T.; Sakuraba, A.; Maeda, Y.; Akasaka, T.; Yoza, K.; Horn, E.; Kato, T.; Liu, M. T. H.; Mizorogi, N.; Kobayashi, K.; Nagase, S. *J. Am. Chem. Soc.* **2005**, *127*, 12500. (b) Yang, H.; Lu, C.; Liu, Z.; Jin, H.; Che, Y.; Olmstead, M. M.; Balch, A. L. *J. Am. Chem. Soc.* **2008**, *130*, 17296.

(3) Stevenson, S.; Mackey, M. A.; Stuart, M. A.; Philips, J. P.; Easterling, M. L.; Chancellor, C. J.; Olmstead, M. M.; Balch, A. L. *J. Am. Chem. Soc.* **2008**, *130*, 11844.

(4) (a) *ADF 2007.01*; Department of Theoretical Chemistry; Vrije Universiteit: Amsterdam. (b) te Velde, G. T.; Bickelhaupt, F. M.; Baerends, E. J.; Guerra, C. F.; Van Gisbergen, S. J. A.; Snijders, J. G.; Ziegler, T. *J. Comput. Chem.* **2001**, *22*, 931.

(5) (a) Becke, A. D. *Phys. Rev. A* **1988**, *38*, 3098. (b) Perdew, J. P. *Phys. Rev. B* **1986**, *33*, 8822.

(6) (a) Klamt, A.; Schuurmann, G. *J. Chem. Soc., Perkin Trans. 2* **1993**, 799. (b) Andzelm, J.; Kolmel, C.; Klamt, A. *J. Chem. Phys.* **1995**, *103*, 9312.

(7) Pye, C. C.; Ziegler, T. *Theor. Chem. Acc.* **1999**, *101*, 396–408.

(8) (a) Chaur, M. N.; Valencia, R.; Rodríguez-Fortea, A.; Poble, J. M.; Echegoyen, L. *Angew. Chem., Int. Ed.* **2009**, *48*, 1425. (b) Pinzón, J. R.; Cardona, C. M.; Herranz, M. A.; Plonska-Brzezinska, M. E.; Palkar, A.; Athans, A. J.; Martin, N.; Rodríguez-Fortea, A.; Poble, J. M.; Bottari, G.; Torres, T.; Gayathri, S. S.; Guldi, D. M.; Echegoyen, L. *Chem.—Eur. J.* **2009**, *15*, 864.

(9) Fernandez, J. A.; Lopez, X.; Bo, C.; De Graaf, C.; Baerends, E. J.; Poble, J. M. *J. Am. Chem. Soc.* **2007**, *129*, 12244.

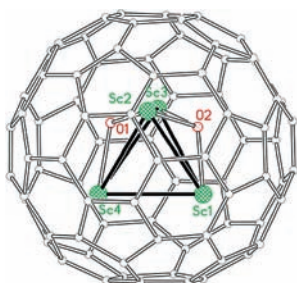


**Figure 1.** Crystallographically determined structure of  $\text{Sc}_4(\mu_3\text{-O})_2@I_h\text{-C}_{80}$  taken from reference 3.

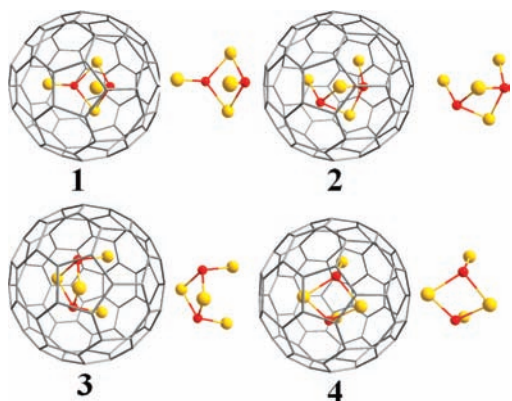


**Figure 2.** Optimized structures of the four lowest-energy orientational isomers of  $\text{Sc}_4(\mu_3\text{-O})_2@I_h\text{-C}_{80}$  analyzed in this work. The structure of the  $\text{Sc}_4(\mu_3\text{-O})_2$  cluster without the surrounding  $I_h\text{-C}_{80}$  unit is also represented to the right of each isomer.

**Table 1.** Most Significant Distances and Relative Energies for the Four Lowest-Energy Orientational Isomers of  $\text{Sc}_4(\mu_3\text{-O})_2@I_h\text{-C}_{80}$ .<sup>a</sup>

	Iso 1	Iso 2	Iso 3	Iso 4	exp.
Sc2–Sc3	2.96	2.94	3.00	2.98	2.95
Sc1–Sc4	3.21	3.25	3.21	3.48	3.12
Sc1,4–Sc2,3 <sup>b</sup>	3.29	3.30	3.25	3.25	3.30
Sc–O <sup>c</sup>	2.01	2.00	2.00	1.98	2.05
Sc...C <sup>d</sup>	2.21	2.25	2.23	2.24	2.02
	2.32	2.32	2.32	2.30	2.28
	2.23	2.22	2.28	2.25	2.21
	2.39	2.31	2.33	2.29	2.24
O...C <sup>e</sup>	2.77	2.79	2.81	2.71	2.72
	2.68	2.68	2.74	2.65	2.56
$\Delta E$	0.0	0.6	0.7	0.8	-

<sup>a</sup>Distances in angstroms (Å) and energies in kcal mol<sup>-1</sup>. <sup>b</sup>Average for the Sc1–Sc2, Sc1–Sc3, Sc4–Sc2, and Sc4–Sc3 distances. <sup>c</sup>Average Sc–O distance. <sup>d</sup>Closest Sc...C distance for each Sc atom. <sup>e</sup>Closest O...C distance for each O atom. For details about isomers 5–9 see Supporting Information.

metal oxide cluster  $\text{Sc}_4(\mu_3\text{-O})_2$  is placed in different orientations inside the  $I_h\text{-C}_{80}$  cage, have been optimized. Relevant data for the four most stable structures, shown in Figure 2, are presented in Table 1 (data for other isomers can be found in the Supporting Information). Energy differences between these orientations are within few kcal mol<sup>-1</sup>. These results indicate that rotation of this rather large cluster inside the  $I_h\text{-C}_{80}$  cage is feasible. This observation is in agreement with the fact that the  $\text{Sc}_4(\mu_3\text{-O})_2$  cluster is disordered over different orientations in the crystalline state.<sup>3</sup> For the lowest energy structure, isomer 1, interatomic distances within the cluster and

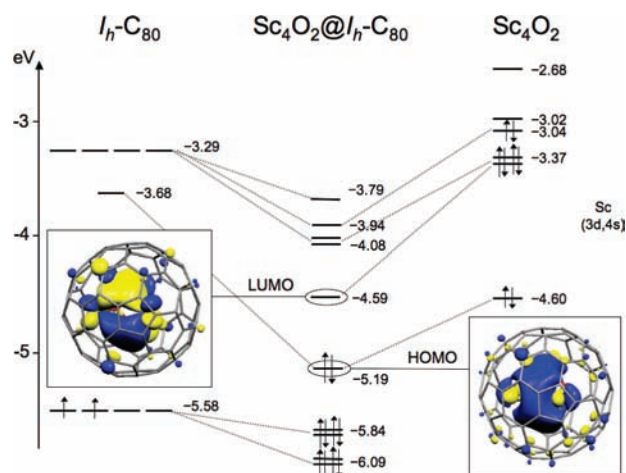


**Figure 3.** Orbital interaction diagram for the lowest-energy isomer (1) of  $\text{Sc}_4(\mu_3\text{-O})_2@I_h\text{-C}_{80}$ . The fragments,  $\text{Sc}_4(\mu_3\text{-O})_2$  and  $I_h\text{-C}_{80}$ , were calculated with the geometry that they have in the EMF.

between the cluster and the cage are well reproduced at our computational level, as can be seen from the data presented in Table 1. Concerning the cluster, two significantly different types of Sc–Sc distances exist: a short distance for the Sc2–Sc3 unit that is bridged by two oxygen atoms and longer distances for the other pairs of scandium atoms. For the cluster...cage interaction, Sc...C distances are comparable to the distances found in  $\text{Sc}_3\text{N}@I_h\text{-C}_{80}$ , as pointed out by Stevenson and Balch.<sup>3</sup> These distances are predicted to be somewhat longer than the experimental values. Moreover, the closest O...C contacts show that there are no unusual interactions between the oxygen atoms and the carbon cage.

Analysis of the electronic structure of  $\text{Sc}_4(\mu_3\text{-O})_2@I_h\text{-C}_{80}$  shows that in contrast to  $\text{Sc}_3\text{N}@I_h\text{-C}_{80}$ , where no metal d electrons are found in the  $\text{Sc}_3\text{N}$  cluster,<sup>10</sup> both the highest occupied molecular orbital (HOMO) and the lowest unoccupied molecular orbital (LUMO) are mainly localized on the Sc atoms of  $\text{Sc}_4(\mu_3\text{-O})_2$  as seen in Figure 3. This electronic structure confirms the mixed-valence-cluster picture proposed by Stevenson and Balch.<sup>3</sup> Inspection of the schematic orbital interaction diagram in Figure 3 clearly shows a formal transfer of six electrons from the three HOMOs of the internal cluster to the  $I_h\text{-C}_{80}$  cage (i.e.,  $[\text{Sc}_4(\mu_3\text{-O})_2]^{6+}@[I_h\text{-C}_{80}]^{6-}$ ), as observed for other stable  $I_h\text{-C}_{80}$ -based endohedral metallofullerenes (EMFs), (i.e.,  $[\text{Sc}_3\text{N}]^{6+}@[I_h\text{-C}_{80}]^{6-}$ ).

The topology of the HOMO, which is delocalized over the four Sc ions (Figure 3), reveals that there are Sc–Sc bonding interactions, especially for those Sc atoms that are connected by less than two O bridges. The presence of two O bridging atoms places the two Sc atoms much closer than those having one or no O bridges, even though the Sc–Sc interaction is somewhat larger for this latter case. The bond distances within the  $\text{Sc}_4(\mu_3\text{-O})_2$  cluster can be easily rationalized from its electronic structure. Before the encapsulation, the four HOMOs of the cluster show mainly (3d, 4s)-Sc contribution (Figure 4). In these four orbitals, delocalized Sc–Sc bonding interactions are present. HOMO-1 and HOMO-2 contain bonding

(10) (a) Campanera, J. M.; Bo, C.; Olmstead, M. M.; Balch, A. L.; Poblet, J. M. *J. Phys. Chem. A* **2002**, *106*, 12356. (b) Campanera, J. M.; Bo, C.; Poblet, J. M. *Angew. Chem., Int. Ed.* **2005**, *44*, 7230.

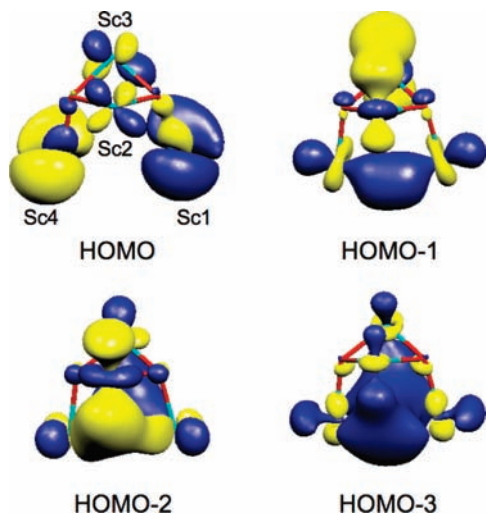


**Figure 4.** Representation of the four highest molecular orbitals for the free  $\text{Sc}_4(\mu_3\text{-O})_2$  cluster.

**Table 2.** Atomic Charges for the Sc Ions in  $\text{Sc}_4(\mu_3\text{-O})_2@I_h\text{-C}_{80}$  and  $\text{Sc}_4(\mu_3\text{-O})_3@I_h\text{-C}_{80}$

	$\text{Sc}_4(\mu_3\text{-O})_2@I_h\text{-C}_{80}$		$\text{Sc}_4(\mu_3\text{-O})_3@I_h\text{-C}_{80}$	
	Mulliken <sup>a</sup>	MDC-q <sup>b</sup>	Mulliken <sup>a</sup>	MDC-q <sup>b</sup>
Sc1	0.64	0.45	1.01	0.95
Sc2	0.89	0.64	0.98	0.87
Sc3	0.89	0.65	1.09	0.67
Sc4	0.60	0.45	1.01	0.92

<sup>a</sup> Mulliken partition. <sup>b</sup> Multipole Derived Charge Analysis (MDC-q).

interactions between Sc1 and Sc4. At the same time, HOMO-1 contains a bonding interaction between Sc2 and Sc3 whereas HOMO-2 shows a somewhat antibonding interaction between these two atoms. HOMO-3, which shows an important bonding interaction between Sc1 and Sc4, becomes the HOMO of the EMF after the encapsulation of the cluster in the carbon cage. Lower-lying cluster orbitals are basically combinations of the (2s, 2p)-O with small contributions of the 3d-Sc orbitals. Because the cluster has lost six electrons that were occupying orbitals with Sc–Sc bonding character, all the Sc–Sc bonds within the cluster are significantly weakened (see Supporting Information). The most important changes are observed for the Sc1–Sc4 distance, which is enlarged 22%. This elongation points out the larger contribution of Sc1 and Sc4 with respect to Sc2 and Sc3 in the three highest-occupied orbitals of the free  $\text{Sc}_4(\mu_3\text{-O})_2$  cluster as well as the fact that the interactions between Sc1 and Sc4 in these three orbitals are all bonding whereas the interaction between Sc2 and Sc3 in one of them is rather antibonding (vide supra). Atomic charges were computed according to the Mulliken partition scheme and Multipole Derived Charge analysis (MDC-q). Both procedures confirm that Sc1 and Sc4 support more electronic density than Sc2 and Sc3 (Table 2). Therefore, molecular orbitals, bond distances, and atomic charges suggest that the endohedral fullerene can be formally described as  $(\text{Sc}_{2,3}^{3+})_2(\text{Sc}_{1,4}^{2+})_2(\text{O}^{2-})_2@I_h\text{-C}_{80}^{6-}$ .

**Redox Properties for  $\text{Sc}_4(\mu_3\text{-O})_2@I_h\text{-C}_{80}$ .** Figure 3 shows that the electronic structure of  $\text{Sc}_4(\mu_3\text{-O})_2@I_h\text{-C}_{80}$  has a very low HOMO–LUMO gap of only

**Table 3.** Computed Redox Properties for the Two Sc-Oxide EMFs

	$\text{Sc}_4(\mu\text{-O})_2@I_h\text{-C}_{80}$	$\text{Sc}_4(\mu\text{-O})_3@I_h\text{-C}_{80}$
OE <sup>a</sup>	+4.59	+5.26
RE <sup>a</sup>	−3.71	−3.65
EC <sup>b</sup>	+0.88	+1.61
H-L <sup>c</sup>	+0.60	+1.49

<sup>a</sup> Reduction (RE) and oxidation (OE) energies at 0 K in *o*-dcb (in eV). <sup>b</sup> Electrochemical gaps computed from RE and OE (in V). <sup>c</sup> HOMO–LUMO gaps (H-L) of the neutral species in *o*-dcb (in eV).

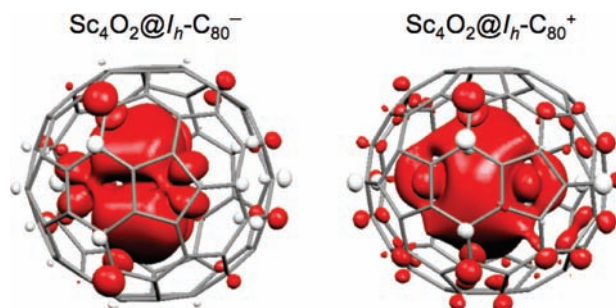


**Figure 5.** Spin densities for the reduced (left) and oxidized (right)  $\text{Sc}_4(\mu_3\text{-O})_2@I_h\text{-C}_{80}$  systems.

**Table 4.** Computed Sc–Sc Distances for Oxidized, Neutral, and Reduced  $\text{Sc}_4(\mu_3\text{-O})_2@I_h\text{-C}_{80}^a$

	oxidized	neutral	reduced
Sc2–Sc3	3.00	2.96	2.94
Sc1–Sc4	3.29	3.20	3.08
Sc1,4–Sc2,3	3.36	3.29	3.22

<sup>a</sup> Distances in angstrom (Å).

0.60 eV, which may be compared with 1.18 eV for  $\text{Sc}_3\text{N}@I_h\text{-C}_{80}$ .<sup>10</sup> The small HOMO–LUMO gap suggests that the EC gap will also be small. The computed redox properties of  $\text{Sc}_4(\mu_3\text{-O})_2@I_h\text{-C}_{80}$  are set out in Table 3. We predict a value of 0.88 V for the EC gap in *o*-dcb. This value, which is a consequence of the small oxidation energy (OE) of  $\text{Sc}_4(\mu_3\text{-O})_2@I_h\text{-C}_{80}$  in *o*-dcb (+4.59 eV), is much smaller than the predicted EC gaps for any of the metal nitride endohedral fullerenes (MNEFs) synthesized so far.<sup>8</sup> The reduction energy, −3.71 eV, is somewhat larger than that found for the prototype of the family of MNEFs,  $\text{Sc}_3\text{N}@I_h\text{-C}_{80}$  (−3.51 eV). Unfortunately,  $\text{Sc}_4(\mu_3\text{-O})_2@I_h\text{-C}_{80}$  has not been electrochemically characterized yet, so comparison of these computed values with experimental results is not possible.

An analysis of the singly occupied molecular orbitals (SOMOs) and the spin densities in the reduced and oxidized states, that is, the anion and cation radicals, confirms that both reduction and oxidation take place in the internal cluster (see Figures 4 and 5). For these radicals, whose ground electronic states are doublets, the shapes of the spin densities for the reduced and oxidized species resemble very much those of the LUMO and HOMO, respectively, of the neutral EMF as comparison of Figures 3, 4, and 5 shows. The changes in the Sc–Sc distances for the oxidized and reduced computational models of  $\text{Sc}_4(\mu_3\text{-O})_2@I_h\text{-C}_{80}$  (Table 4) also confirm the presence of direct Sc–Sc bonding interactions. The effect of removing one electron from the HOMO is less

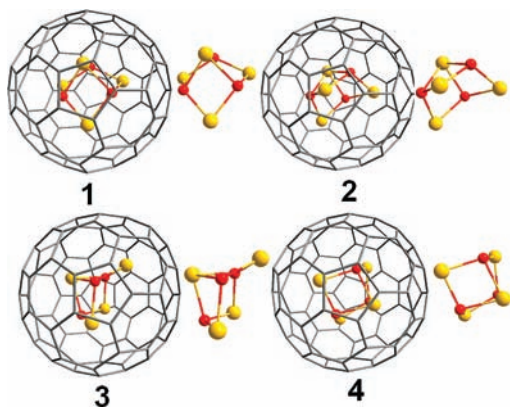


**Figure 6.** Optimized structures of the four lowest-energy orientational isomers of  $\text{Sc}_4(\mu_3\text{-O})_3@I_h\text{-C}_{80}$  analyzed in this work. The structure of the  $\text{Sc}_4(\mu_3\text{-O})_3$  cluster without the surrounding  $I_h\text{-C}_{80}$  unit is also represented to the right of each isomer.

important on the Sc2–Sc3 distance and larger on the Sc1–Sc4 one. The shortening when one electron is added also agrees with the Sc–Sc bonding character of the LUMO. We could describe this situation as a four-center, two-electron interaction. The four Sc ions, however, do not contribute exactly the same amount to the HOMO, as observed for the three HOMOs of the free  $\text{Sc}_4(\mu_3\text{-O})_2$  cluster (vide supra).

**Structure and Electronic Properties of  $\text{Sc}_4(\mu_3\text{-O})_3@I_h\text{-C}_{80}$ .** For the structures with the  $\text{Sc}_4\text{O}_3\text{C}_{80}$  formula, we have found that  $\text{Sc}_4(\mu_3\text{-O})_3@I_h\text{-C}_{80}$ , the EMF with the additional O atom in the cluster, is much more stable (by around  $115 \text{ kcal mol}^{-1}$ ) than  $\text{Sc}_4(\mu_3\text{-O})_2@I_h\text{-C}_{80}\text{O}$ , the EMF where the extra O atom is present as an exohedral epoxide group (see the Supporting Information for different isomers of  $\text{Sc}_4(\mu_3\text{-O})_2@I_h\text{-C}_{80}\text{O}$  and their energies relative to  $\text{Sc}_4(\mu_3\text{-O})_3@I_h\text{-C}_{80}$ ). For  $\text{Sc}_4(\mu_3\text{-O})_2@I_h\text{-C}_{80}\text{O}$ , the frontier molecular orbitals are analogous to those found for  $\text{Sc}_4(\mu_3\text{-O})_2@I_h\text{-C}_{80}$  with a small HOMO–LUMO gap of  $0.68 \text{ eV}$ . From a stability criterion, we propose  $\text{Sc}_4(\mu_3\text{-O})_3@I_h\text{-C}_{80}$  to be the structure for  $\text{Sc}_4\text{O}_3\text{C}_{80}$ . It is important to note that the energy differences between the 12 orientational isomers of  $\text{Sc}_4(\mu_3\text{-O})_3@I_h\text{-C}_{80}$  that we have computed are within less than  $5 \text{ kcal mol}^{-1}$ , thus indicating that the seven-atom  $\text{Sc}_4(\mu_3\text{-O})_3$  cluster is also able to rotate inside the  $I_h\text{-C}_{80}$  cage (see Figure 6 and Table 5). Interatomic distances for the four lowest-energy isomers are presented in Table 5. Similarly to  $\text{Sc}_4(\mu_3\text{-O})_2@I_h\text{-C}_{80}$ , the Sc–Sc distances for those pairs of Sc atoms that are bonded by two O bridges (Sc1–Sc2, Sc2–Sc3 and Sc2–Sc4, see Supporting Information, Figure S8) are shorter (around  $3 \text{ \AA}$ ) than the distances for those pairs of Sc ions bonded by only one O bridge (Sc1–Sc3, Sc1–Sc4, and Sc3–Sc4, around  $3.4 \text{ \AA}$ ). Interestingly, this latter distance is longer than in the case of  $\text{Sc}_4(\mu_3\text{-O})_2@I_h\text{-C}_{80}$  ( $3.43$  vs  $3.27 \text{ \AA}$ ). The Sc–O as well as the closest Sc...C and O...C distances do not show important differences when compared to  $\text{Sc}_4(\mu_3\text{-O})_2@I_h\text{-C}_{80}$ . Thus, the presence of an additional O atom in the interior of the fullerene does not lead to significant strain between the cluster and the cage.

The electronic structure of  $\text{Sc}_4(\mu_3\text{-O})_3@I_h\text{-C}_{80}$  is, however, different from that of  $\text{Sc}_4(\mu_3\text{-O})_2@I_h\text{-C}_{80}$ , as shown in the orbital interaction diagram of Figure 7. Within the

**Table 5.** Most Significant Distances and Relative Energies for the Four Lowest-Energy Orientational Isomers of  $\text{Sc}_4(\mu_3\text{-O})_3@I_h\text{-C}_{80}$ <sup>a</sup>

	Iso 1	Iso 2	Iso 3	Iso 4
Sc–Sc <sup>b</sup>	2.98	2.98	2.98	2.99
	3.45	3.44	3.45	3.42
Sc–O <sup>c</sup>	1.99	1.99	1.99	1.99
Sc...C <sup>d</sup>	2.25	2.25	2.25	2.26
	2.36	2.48	2.40	2.40
	2.24	2.23	2.27	2.24
	2.28	2.25	2.25	2.32
O...C <sup>e</sup>	2.66	2.60	2.67	2.68
	2.64	2.71	2.67	2.79
	2.69	2.68	2.74	2.68
$\Delta E$	0.0	0.8	0.9	1.2

<sup>a</sup> Distances in angstrom ( $\text{\AA}$ ) and energies in  $\text{kcal mol}^{-1}$ . <sup>b</sup> First row: average Sc–Sc distance for the Sc pairs that have two O atoms as bridges; second row: average Sc–Sc distance for Sc pairs that have only one O atom as bridge. <sup>c</sup> Average Sc–O distance. <sup>d</sup> Closest Sc...C distance for each Sc atom. <sup>e</sup> Closest O...C distance for each O atom. For details about isomers 5–12 see Supporting Information.

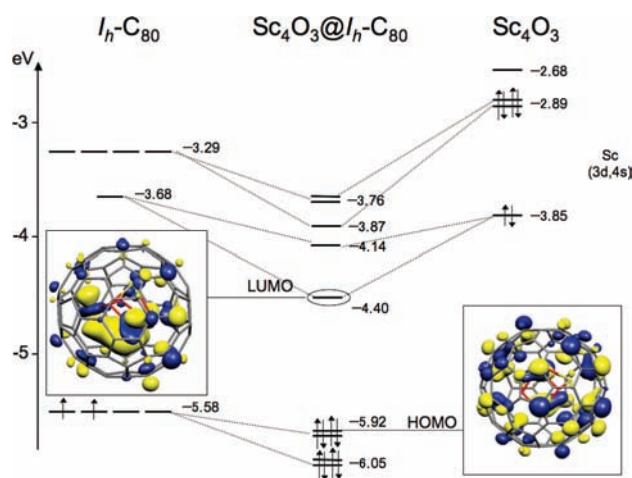


**Figure 7.** Orbital interaction diagram for the lowest-energy isomer (1) of  $\text{Sc}_4(\mu_3\text{-O})_3@I_h\text{-C}_{80}$ . The fragments,  $\text{Sc}_4(\mu_3\text{-O})_3$  and  $I_h\text{-C}_{80}$ , were calculated with the geometry that they have in the EMF.

ionic model, we can consider  $\text{Sc}_4(\mu_3\text{-O})_3@I_h\text{-C}_{80}$  as  $(\text{Sc}^{3+})_4(\text{O}^{2-})_3@I_h\text{-C}_{80}^{6-}$ . Because the cluster contains a third oxide ion, the four Sc ions have formal charges of +3. Each Sc atom has lost all of its d electrons, resulting in a cluster that contains four completely oxidized metal centers as compared to the mixed valence cluster present in  $\text{Sc}_4(\mu_3\text{-O})_2@I_h\text{-C}_{80}$ . The atomic charges in Table 2 clearly show that the addition of a third oxide entails a loss of charge density in particular for atoms Sc1 and Sc4, which increase their formal oxidation states from  $2+$  to  $3+$ . For  $\text{Sc}_4(\mu_3\text{-O})_3@I_h\text{-C}_{80}$ , the HOMO is localized on the metal cluster (see Figure 7), as occurs for  $\text{Sc}_3\text{N}@I_h\text{-C}_{80}$ .<sup>10</sup> Since there are no bonding interactions between the Sc atoms that only have an O bridge, the corresponding Sc–Sc distances are larger (see Tables 1 and 5). The three HOMOs of the free  $\text{Sc}_4(\mu_3\text{-O})_3$  cluster show delocalized Sc–Sc bonding interactions, similar to  $\text{Sc}_4(\mu_3\text{-O})_2$  (see Supporting Information). As a consequence of the lower energy of the HOMO as compared to  $\text{Sc}_4(\mu_3\text{-O})_2@I_h\text{-C}_{80}$ , the computed OE for  $\text{Sc}_4(\mu_3\text{-O})_3@I_h\text{-C}_{80}$  in *o*-dcb is now much larger ( $+5.26 \text{ eV}$ ) and compares very well with that of  $\text{Sc}_3\text{N}@I_h\text{-C}_{80}$  ( $+5.21 \text{ eV}$ ), in good agreement with the

fact that their HOMOs are very similar.<sup>8,10</sup> Accordingly, the HOMO–LUMO and the EC gaps are now much larger, 1.49 eV and 1.61 V, respectively. For comparison, the EC gap for  $\text{Sc}_3\text{N}@I_h\text{-C}_{80}$  is predicted to be 1.70 V.

### Conclusions

The electronic structures for the two title complexes have been discussed. The structural parameters of the observed  $\text{Sc}_4(\mu_3\text{-O})_2@I_h\text{-C}_{80}$  were well reproduced by DFT methods, the endohedral metallofullerene being formed by the formal transfer of six electrons from the cluster to the carbon cage. The HOMO and LUMO of the EMF reveal the presence of some  $\text{Sc}\cdots\text{Sc}$  interaction between the four metal atoms. Analysis of atomic charges support the mixed-valence cluster picture  $(\text{Sc}_{2,3}^{3+})_2(\text{Sc}_{1,4}^{2+})_2(\text{O}^{2-})_2@I_h\text{-C}_{80}^{6-}$ . The fullerene encapsulating the  $\text{Sc}_4\text{O}_3$  cluster,  $\text{Sc}_4(\mu_3\text{-O})_3@I_h\text{-C}_{80}$ , was computed to be much more stable ( $> 115 \text{ kcal mol}^{-1}$ ) than the isomer with an external epoxide,  $\text{Sc}_4(\mu_3\text{-O})_2@I_h\text{-C}_{80}\text{O}$ .

Thus, the  $\text{Sc}_4(\mu_3\text{-O})_2@I_h\text{-C}_{80}\text{O}$  structure is not a viable option for  $\text{Sc}_4\text{O}_3\text{C}_{80}$ . In  $\text{Sc}_4(\mu_3\text{-O})_3@I_h\text{-C}_{80}$  all of the Sc atoms are in oxidation state of 3+. Theoretical electrochemical studies for  $\text{Sc}_4(\mu_3\text{-O})_2@I_h\text{-C}_{80}$  suggest that this compound should exhibit a very small electrochemical gap. In contrast,  $\text{Sc}_4(\mu_3\text{-O})_3@I_h\text{-C}_{80}$  is predicted to have a more conventional behavior with a larger electrochemical gap.

**Acknowledgment.** This work was supported by the Spanish MCINN [CTQ2008-06549-C02-01/BQU and the Ramón y Cajal Program (ARF)] and by the DURSI of the Generalitat de Catalunya (2005SGR-00104). R.V. thanks the Generalitat de Catalunya for a doctoral fellowship.

**Supporting Information Available:** Tables and figures showing details of the computational results. This material is available free of charge via the Internet at <http://pubs.acs.org>.